

A TCT and annealing study on Magnetic Czochralski silicon detectors irradiated with neutrons and 24 GeV/c protons

Nicola Pacifico^{a,*}, Donato Creanza^a, Mauro de Palma^a, Norman Manna^a,
Gregor Kramberger^b, Michael Moll^c

^a Università degli Studi di Bari, Italy

^b Jozef Stefan Institut, Ljubljana, Slovenia

^c CERN, Geneva (CH), Switzerland

ARTICLE INFO

Available online 8 August 2009

Keywords:

TCT
Annealing
MCz
Silicon detectors
RD50

ABSTRACT

Silicon diodes (pad detectors) were irradiated with 24 GeV/c protons at the CERN PS IRRAD1 facility and with neutrons at the TRIGA reactor in Ljubljana (Slovenia). The diodes were realized on Magnetic Czochralski (MCz) grown silicon, of both n- and p-type. After irradiation, an annealing study with CV measurements was performed on 24 GeV/c proton irradiated detectors, looking for hints of type inversion after irradiation and during annealing. Other pad detectors were studied using the TCT (transient current technique), to gather information about the field profile in the detector bulk and thus about the effective space charge distribution within it.

© 2009 Elsevier B.V. All rights reserved.

1. Introduction

Silicon detectors are currently used for the construction of the tracking systems of many High Energy Physics experiments, such as those at the Large Hadron Collider at CERN. The current generation of trackers is built using Float Zone (FZ) silicon. The FZ growing technique allows for a good crystalline purity, which results in homogeneous ingots with a very high resistivity ($10^4 \Omega/\text{cm}$). The tracking system is nevertheless subject to high levels of radiation, up to 10^{15} fast hadrons per cm^2 . The possible upgrade scenario for the LHC (super-LHC) [1] is aiming for an increase in luminosity by a factor 10, thus making the radiation damage issue a critical factor. At those levels of radiations, Float Zone silicon shows its limits, with a fast increase of the full depletion voltage and a loss in charge collection efficiency, due to the formation of deep levels in the bulk that act as trapping centers for the carriers, thus reducing the signal read at the electrodes. The leakage current also increases dramatically with irradiation, along with the power dissipation of the detector, which becomes a critical issue. The most recent studies are looking in the direction of other silicon growth techniques, such as the Magnetic Czochralski (MCz). It has been shown that high levels of oxygen (naturally present in MCz silicon) have beneficial effects in terms of radiation hardness of the detector [2].

The NIEL hypothesis [3] allows for rescaling the damage produced by different kinds of particles with different energies to

a reference fluence, by means of a scaling factor k (hardness factor). The NIEL hypothesis describes correctly the proportional increase of the leakage current density with fluence for charged hadrons with different energies. The proportionality factor, called α , was found to be independent from the used silicon material with different resistivity, conduction type (n- and p-type) and oxygen content [4]. Other effects, however, like the change of the effective doping concentration and the decrease of the effective trapping times cannot be rescaled in the same fashion for all silicon materials and particle types [5,6].

It has been observed that in MCz as well as in FZ silicon detectors, irradiation with hadrons produces two different regions of space charge [7]. A region with positive space charge dominates close to the p^+ contact, while negative space charge dominates close to the n^+ contact. These two space charge regions affect the shape of the current pulse induced after generation of non-equilibrium carriers, which shows two peaks corresponding to the high fields associated with the two different space charge regions.

In the present work, p- and n-type MCz diodes irradiated with reactor neutrons and 24 GeV/c protons were studied to further investigate this *double junction* effect [8]. Where n_{eq} fluences are shown, the NIEL scaling hypothesis was used, using a scaling factor $k = 0.62$ [9].

2. Studied structures and irradiation

In this work PAD detector structures produced from MCz n- and p-type silicon were studied. The wafers were produced

* Corresponding author.

E-mail address: Nicola.Pacifico@cern.ch (N. Pacifico).

Table 1
Investigated structures.

Producer	Type of silicon	Active area (mm ²)	Irradiation	Experimental technique
SMART	n and p	13.7	Protons	TCT, CV/IV
HIP	n	25	Protons	CV/IV
HIP	p	25	Neutrons	TCT
Micron, CNM	n	25	Neutrons	TCT

by Okmetic Ltd. and processed by four different institutes: ITC/IRST—Trento (Italy—processing performed on behalf of the SMART collaboration), Helsinki Institute of Physics (HIP), Centro Nacional de Microelectronica (CNM, Barcelona) and Micron Semiconductors (UK). A list of the structures is shown in Table 1.

All of the diodes studied in this work were provided with an optical window on the non-ohmic contact, allowing e–h pair generation by light on this side of the detector. Some of the diodes (those processed by HIP and Micron) had a patterning on the metallization of the ohmic contact of the diode, allowing for illumination also from this side. All diodes had multiple guard rings. The innermost guard ring was connected to ground during all presented measurements.

The irradiation of the structures was performed at the CERN PS IRRAD1 facility for 24 GeV/c protons and at the Ljubljana TRIGA reactor for neutrons. The maximum irradiation fluence were, respectively, 2.4×10^{15} p/cm² and 8×10^{14} n/cm². The samples were irradiated at room temperature and stored, afterwards, at -20°C to prevent uncontrolled annealing.

3. CV characterization

The CV method [3] was used to determine the depletion voltage of the diodes irradiated with 24 GeV/c protons. Studies performed on Standard Float Zone silicon [3] show that the annealing of irradiated silicon can be divided into two stages. At the beginning there is a partial removal of the negative space charge introduced by irradiation (beneficial annealing), followed by a subsequent introduction of negative space charge (long term or ‘reverse’ annealing). The beneficial annealing behavior of the depletion voltage allows to distinguish between n-type substrates and p-type ones. In a p-type device an introduction of negative space charge results in an increase in V_{dep} while in a n-type device the V_{dep} decreases. The annealing may be accelerated by keeping the silicon at elevated temperatures (usually 60 or 80 °C). The acceleration factor may be calculated through an Arrhenius relation [3]. In the present study annealing has been carried out by heating the samples in an oven, to a temperature of 80 °C. After annealing, the samples were always kept for at least 12 h at room temperature in a dark environment, to allow for the de-excitation of bistable levels [10].

The annealing study has been conducted on 24 GeV/c proton irradiated HIP (MCz-n) and SMART (both MCz-n and MCz-p) samples. The plot V_{dep} vs. annealing time is shown in Fig. 1 for the HIP MCz-n set and in Fig. 2 for the SMART MCz-n one. For depletion voltages above 1000 V, an extrapolation was operated for the depletion voltage, by imposing the geometrical capacitance of the detector (known). All the samples studied show an n-type annealing behavior, with V_{dep} rising slightly with beneficial annealing and then falling again with reverse annealing. All samples, with the exception of the least irradiated HIP diode, show an increase of V_{dep} after about 500 min at 80 °C indicating that the effective space charge is negative for these samples at this annealing stage.

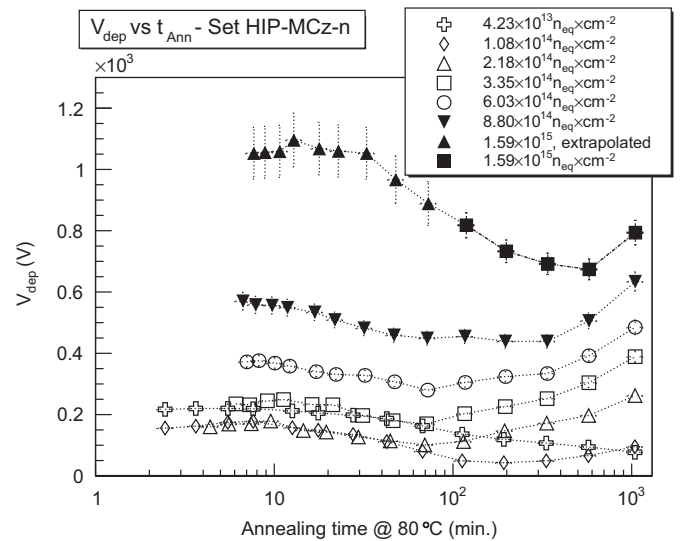


Fig. 1. V_{dep} vs. t_{ann} for the set of HIP MCz-n diodes with 24 GeV/c protons irradiation.

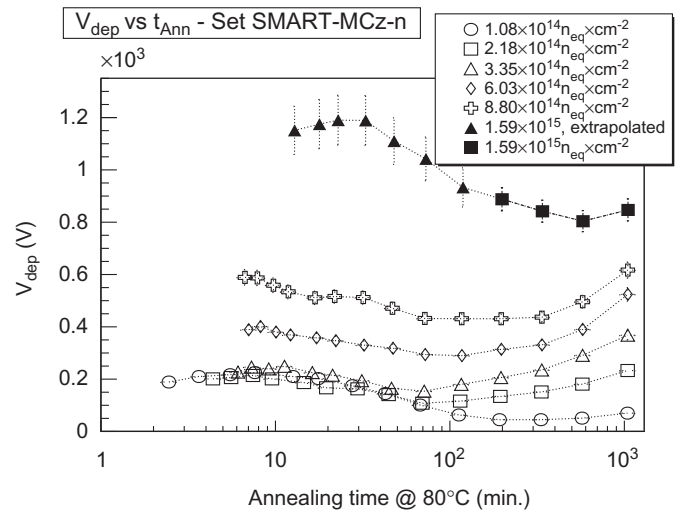


Fig. 2. V_{dep} vs. t_{ann} for the set of SMART MCz-n diodes set with 24 GeV/c protons irradiation.

The same plot is shown in Fig. 3 for SMART MCz-p samples. The annealing behavior for the three least irradiated diodes is p-type like, with V_{dep} falling during beneficial annealing and then rising back during reverse annealing. However, the most irradiated diode (1.6×10^{15} n_{eq}/cm²) shows an n-like annealing behavior, with a curve that is comparable to those of MCz-n diodes irradiated at the same fluence. There are thus indications of dominant space charge sign inversion for MCz-p silicon from p- to n-type at this fluence.

Moreover, MCz-p devices are characterized by a sudden drop in the depletion voltage in the very first stage of annealing, which in

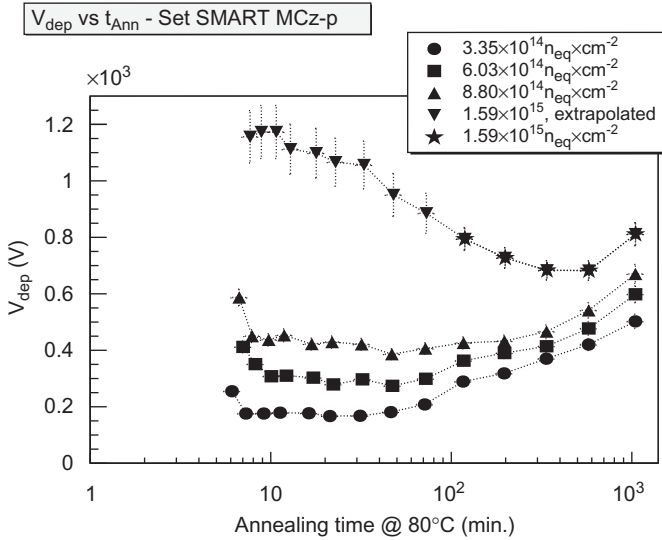


Fig. 3. V_{dep} vs. t_{ann} for the set of SMART MCz-p diodes with 24GeV/c protons irradiation.

MCz-n is not observed. This difference could be related to some effect concerning the p-type boron dopants within the detector bulk. Either, immediately after irradiation, they form some unstable negatively charged complex defects that anneal very quickly into other neutral defects, or the boron, still present in the detector bulk, is neutralized during this short term annealing by some irradiation related defects.

4. TCT measurements

The TCT (Transient Current Technique) has been used to study the electric field profile within the reverse polarized diode. A red laser (670 μm) has been used to create optically generated free carriers within the first few microns from the surface of the device. The pulse length for the laser was 2 ns. One type of carrier is immediately transported to the nearby electrode while the other travels through the depleted detector bulk toward the opposite electrode (holes drift to p⁺ electrode and electrons to n⁺ electrode). Since only one carrier type contributes to the induced current we speak of electron (p⁺ illumination) or hole injection (n⁺ illumination). While travelling through the detector, the speed of the carriers, and thus the induced current, depends on the intensity of the local field by means of the relations

$$\mathbf{v} = \mu \mathbf{E} \quad (1)$$

$$I(t) = \pm \frac{q_0}{W} \cdot v \quad (2)$$

where W is the thickness of the detector and v the drift velocity of the carriers.

Thus, the induced current will be higher in the regions where the carriers drift in a stronger electric field. In a detector with positive space charge (n-type bulk), the induced current pulse plotted against drift time shows a single peak immediately after the charge (electrons in this case) injection. After change in dominant space charge (SCSI) the peak in the induced current appears later, when the drifting carriers reach the high electric field region at the other side of the detector (the main junction has moved).

Previous studies have shown that after irradiation at very high fluences above about $10^{14} n_{eq}$ MCz silicon diodes start to show double-junction effects, i.e. the presence of two space charge

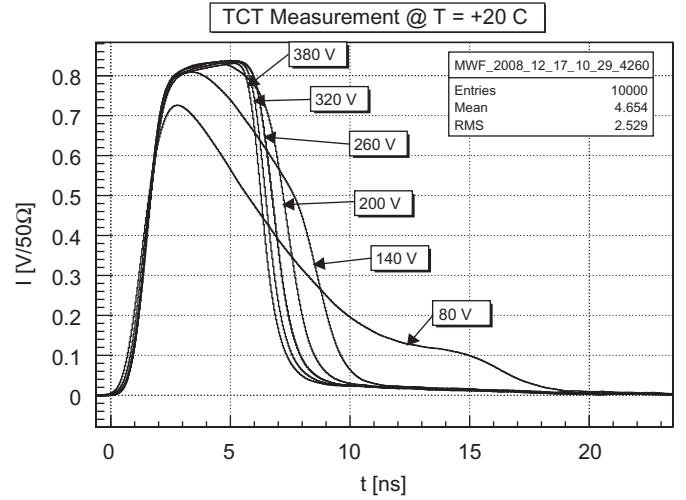


Fig. 4. Induced current after electron injection (p⁺ illumination) for the MCz-n detector irradiated with $1 \times 10^{14} n/cm^2$.

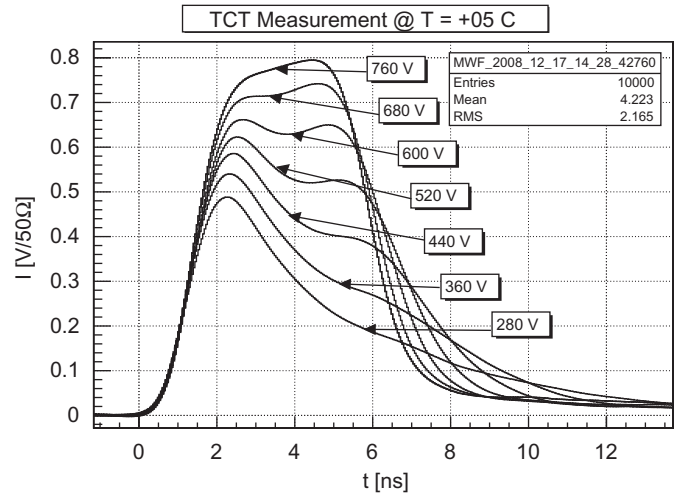


Fig. 5. Induced current after electron injection (p⁺ illumination) for the MCz-n detector irradiated with $8.80 \times 10^{14} n/cm^2$.

regions, one with positive charge (adjacent to the p⁺ contact) and the other with negative space charge (near the n⁺ contact). This behavior is seen in both n- and p-type devices. One possible explanation is the activation of two (or more) different kinds of charged defects in the proximity of the two contacts, due to the strong band bending that occurs in these regions [7.11]: close to the contacts, holes and electrons are trapped within deep defects induced in the bulk by irradiation. This produces two regions with an intense electric field, thus resulting in the formation of a double peak in the current pulse shape.

In the present study, TCT was used on both MCz-p and MCz-n silicon. Unless otherwise stated, all samples have been annealed for 5 min at 80 °C. Irradiation of MCz silicon detectors with neutrons introduces negative space charge in the detector bulk. This can be seen from Figs. 4 and 5 for MCz-n devices. In Fig. 4, even a relatively low dose of neutrons produces a negative space charge region on the ohmic side of the diode which can easily be seen from the current pulse shape for $V_{bias} \geq 280$ V. Irradiation at higher fluences makes this second peak predominant over the first one. The effect is the same as observed in MCz-p silicon (Fig. 6). In this case the negative space charge increases close the main junction, even if a small electric field close to the ohmic contact

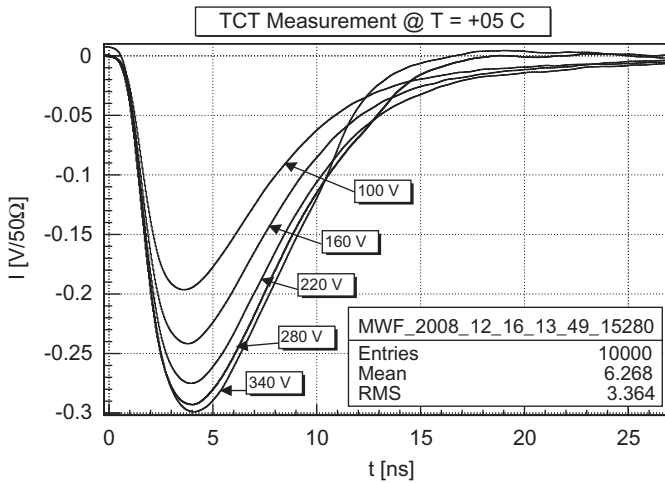


Fig. 6. Induced current after hole injection (n^+ illumination) for the MCz-p detector irradiated with 1×10^{14} n/cm².

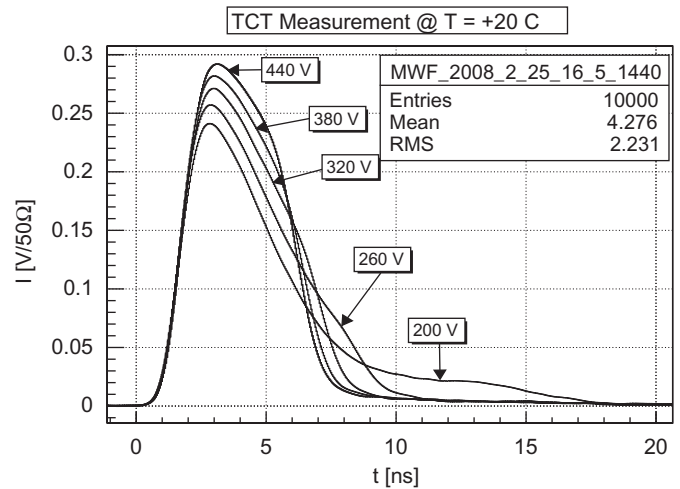


Fig. 8. Induced current after electron injection (p^+ illumination) for the MCz-n detector irradiated with 1.7×10^{14} p/cm².

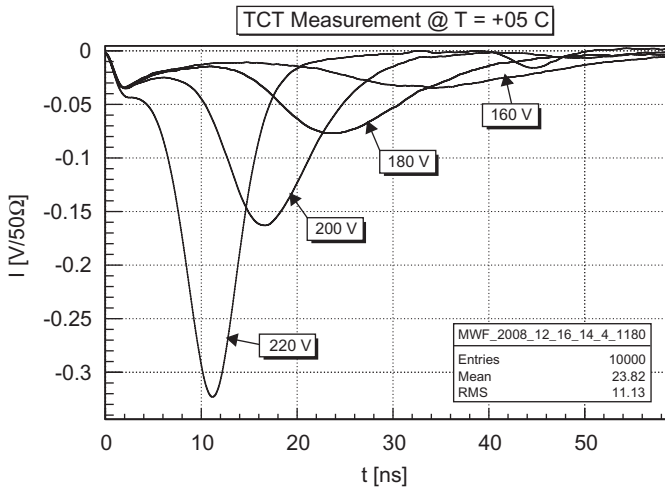


Fig. 7. Induced current after electron injection (p^+ illumination) for the MCz-p detector irradiated with 1×10^{14} n/cm².

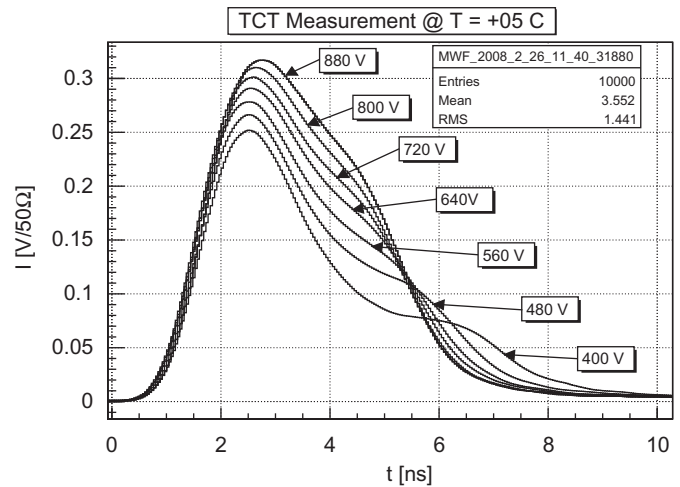


Fig. 9. Induced current after electron injection (p^+ illumination) for the MCz-n detector irradiated with 14×10^{14} p/cm².

forms due to a positive space charge; this can only be observed by illuminating the ohmic contact (Fig. 7—it should be noted here that the absolute height of peaks between illumination from the two sides is not directly comparable due to the different apertures of the silicon exposed to the laser light while illuminating the two contacts).

The situation is radically different after irradiation with 24 GeV/c protons. In this case, also at very low fluences, a pronounced region of high field can be observed close to the p^+ contact, thus indicating the presence of positive space charge in this region (see Figs. 8 and 9). This effect can also be seen in MCz-p silicon, where a saddle in the current pulse shape is visible even at very low fluences (Figs. 10 and 11). Also in this case there is, however, the introduction of negative space charge near the n^+ junction, as can be seen from Figs. 8 and 9. At higher fluences (Figs. 12 and 13), the negative space charge is still visible, though to obtain information about the dominant peak, the pulses should be corrected for trapping. However, at the high fluences studied in this work, the uncertainty associated to the trapping times determined is too high and provides inconsistent results [12]. No estimation of trapping time is hence proposed in this work.

Diodes from the SMART set, irradiated with 24 GeV/c protons, were annealed at 80 °C for 1000 min, to make the TCT measurements

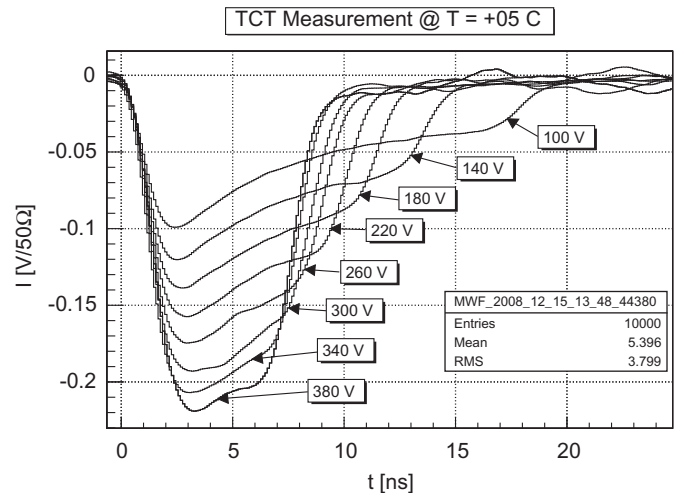


Fig. 10. Induced current after hole injection (n^+ illumination) for the MCz-p detector irradiated with 1.7×10^{14} p/cm².

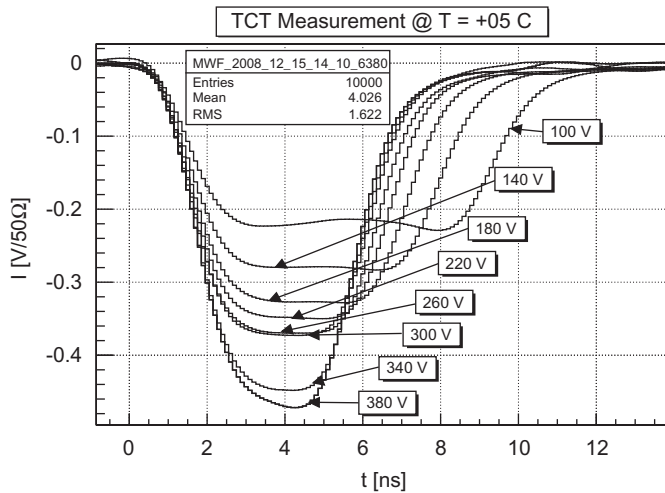


Fig. 11. Induced current after electron injection (p^+ illumination) for the MCz-p detector irradiated with $1.7 \times 10^{14} \text{ p/cm}^2$.

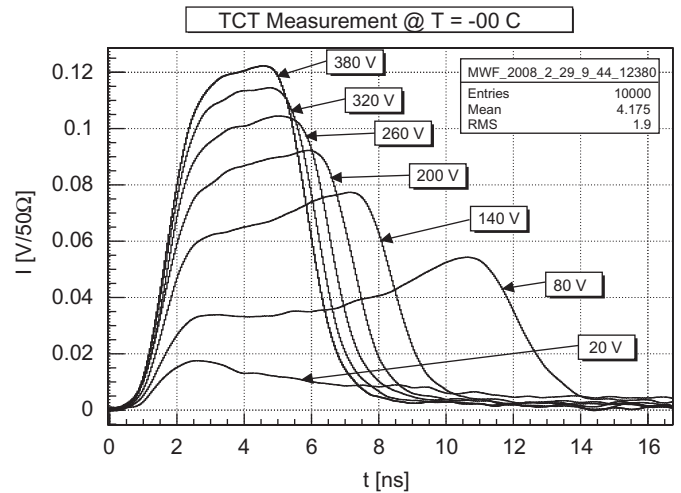


Fig. 14. Induced current after electron injection (p^+ illumination) for the MCz-n detector irradiated with $1.7 \times 10^{14} \text{ p/cm}^2$ after 1000 min of annealing at 80 °C.

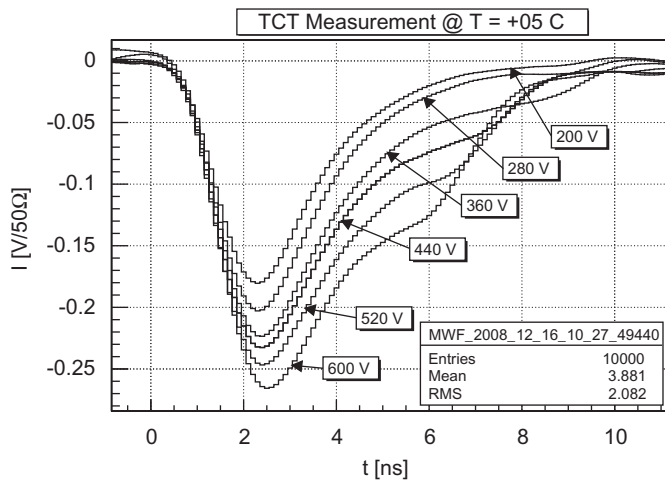


Fig. 12. Induced current after hole injection (n^+ illumination) for the MCz-p detector irradiated with $14 \times 10^{14} \text{ p/cm}^2$.

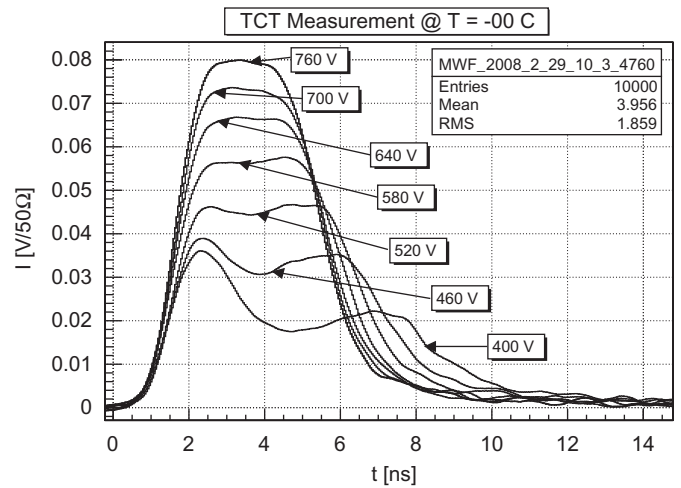


Fig. 15. Induced current after electron injection (p^+ illumination) for the MCz-n detector irradiated with $14 \times 10^{14} \text{ p/cm}^2$ after 1000 min of annealing at 80 °C.

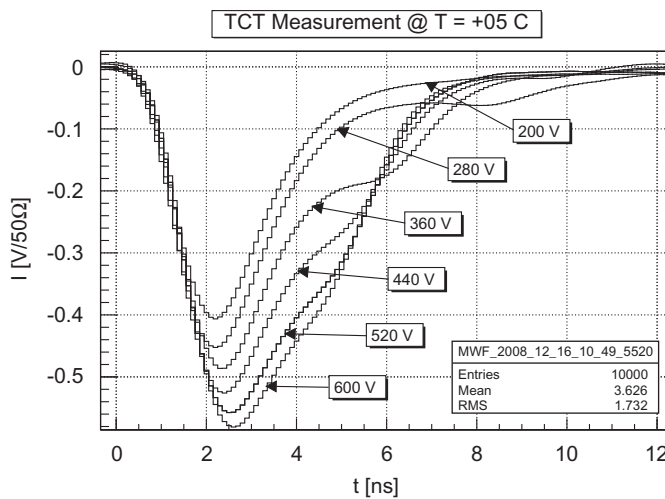


Fig. 13. Induced current after electron injection (p^+ illumination) for the MCz-p detector irradiated with $14 \times 10^{14} \text{ p/cm}^2$.

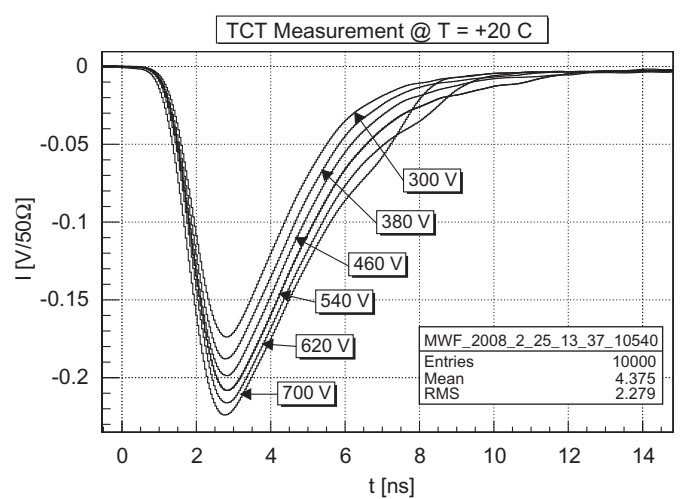


Fig. 16. Induced current after hole injection (n^+ illumination) for the MCz-p detector irradiated with $1.7 \times 10^{14} \text{ p/cm}^2$ after 1000 min of annealing at 80 °C.

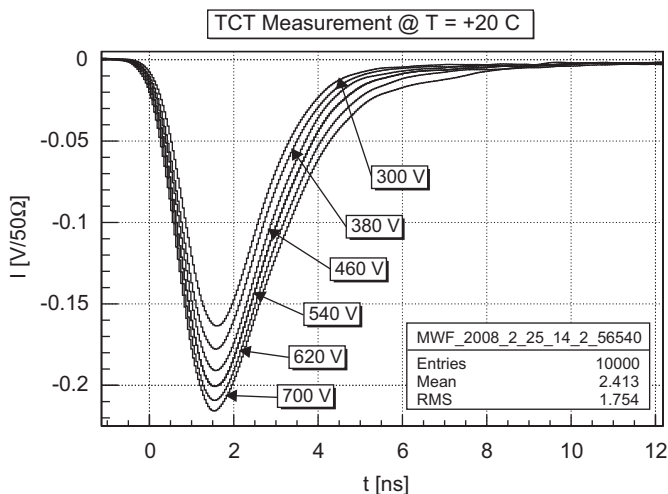


Fig. 17. Induced current after hole injection (n^+ illumination) for the MCz-p detector irradiated with 14×10^{14} p/cm² after 1000 min of annealing at 80 °C.

comparable with the last point from the CV study (Figs. 2 and 3). MCz-n diodes actually show a junction on the ohmic side that rises with annealing (Figs. 14 and 15, as compared to Figs. 8 and 9).

For the MCz-p samples, on the other hand, the electric field at the n^+ junction is becoming predominant over the electric field on the ohmic junction during annealing (Figs. 16 and 17).

5. Discussion of results

In this work, results on neutron and 24 GeV/c proton irradiated n- and p-type MCZ silicon diodes produced by four different producers have been presented using the CV and TCT methods. Irradiation with neutrons introduces negative space charge close to the n^+ contact, moving the main junction on this side of the detector. The effect is so dramatic that it can be seen from TCT curves even without trapping correction. On the other hand, annealing curves suggest that, following irradiation with 24 GeV/c protons, positive space charge is introduced within the detector

bulk, resulting in even higher electric field strength in proximity of the p^+ contact. For the highest fluence studied here (1.6×10^{15} n_{eq}/cm²), this positive space charge ultimately leads the MCz-p diode to show an n-type annealing behavior, suggesting that the main junction has moved on the ohmic contact side. This conclusion is supported by the TCT curves, where the junction in proximity of the p^+ contact has been shown to increase with fluence, though it was not possible to perform a TCT on the highest irradiated sample due to the very high depletion voltage (> 1200 V).

To obtain clear information from TCT measurements about the dominating junction, the pulses should be corrected for trapping. However, at the present time, no precise trapping time measurements at these fluences are available.

Acknowledgments

We would like to thank Maurice Glaser, for the support at the 24 GeV/c irradiation facility at CERN and the people at the TRIGA reactor in Ljubljana, which have made the irradiation campaigns possible. This work was performed in the frameworks of the SMART and RD50 Collaborations.

References

- [1] F. Gianotti, et al., Physics potential and experimental challenges of the LHC luminosity upgrade, hep-ph/0204087, 2005.
- [2] I. Pintilie, M. Buda, E. Fretwurst, F. Hönniger, G. Lindström, J. Stahl, Nucl. Instr. and Meth. A 552 (2005) 56.
- [3] M. Moll, Ph.D. Thesis—DESY-THESIS—1999-040.
- [4] M. Moll, E. Fretwurst, G. Lindström, Nucl. Instr. and Meth. A 426 (1999) 87.
- [5] G. Kramberger, V. Cindro, I. Mandić, M. Mikuž, Nucl. Instr. and Meth. A 579 (2007) 762.
- [6] S. Dittongo, L. Bosisio, D. Contarato, G. D'Auria, E. Fretwurst, J. Härkönen, G. Lindström, E. Tuovinen, Nucl. Instr. and Meth. A 546 (2005) 300.
- [7] E. Verbitskaya, V. Eremin, Z. Li, J. Härkönen, M. Bruzzi, Nucl. Instr. and Meth. A 583 (2007) 77.
- [8] V. Eremin, Z. Li, I. Iljashenko, Nucl. Instr. and Meth. A 360 (1994) 458.
- [9] M. Glaser, L. Durieu, F. Lemeilleur, M. Tavlet, C. Leroy, P. Roy, Nucl. Instr. and Meth. A 426 (1999) 72.
- [10] D. Creanza, D. Giordano, M. de Palma, L. Fiore, N. Manna, S. My, V. Radicci, P. Tempesta, Nucl. Instr. and Meth. A 530 (2004) 128.
- [11] D. Menichelli, M. Scaringella, S. Miglio, M. Bruzzi, Z. Li, E. Fretwurst, I. Pintilie, et al., Nucl. Instr. and Meth. A 530 (2004) 139.
- [12] V. Cindro, G. Kramberger, M. Lozano, I. Mandić, M. Mikuž, G. Pellegrini, J. Pulko, M. Ullan, M. Zavrtanik, Nucl. Instr. and Meth. A 599 (2009) 60.